Dyes and Pigments 83 (2009) 81–87

Contents lists available at ScienceDirect

Dyes and Pigments

journal homepage: www.elsevier.com/locate/dyepig

Cationic porphyrin–anthraquinone dyads: Modes of interaction with G-quadruplex DNA

Ping Zhao [a], Lian-Cai Xu [b], Jin-Wang Huang [a,c,*], Bo Fu [a], Han-Cheng Yu [a], Liang-Nian Ji [a,c]

[a] MOE Laboratory of Bioinorganic and Synthetic Chemistry, School of Chemistry and Chemical Engineering, Sun Yat-Sen University, Xingangxi Road, Guangzhou 510275, PR China
[b] Center for Computational Quantum Chemistry, South China Normal University, Guangzhou 510631, PR China
[c] State Key Laboratory of Optoelectronic Material and Technologies, Sun Yat-Sen University, Xingangxi Road, Guangzhou 510275, PR China

ARTICLE INFO

Article history:
Received 18 November 2008
Received in revised form
19 March 2009
Accepted 19 March 2009
Available online 5 April 2009

Keywords:
Porphyrin–anthraquinone dyads
Quadruplex DNA
Interaction
SERS
Job plot
Stabilization

ABSTRACT

The interaction of a parallel, guanine quadruplex DNA with four, cationic porphyrin–anthraquinone dyads which comprise bridging linkages of differing lengths, was investigated for the first time. Using a combination of absorption and fluorescence titration, surface-enhanced Raman spectroscopy and induced circular dichroism spectroscopy as well as Job plot, it was found that the porphyrin and anthraquinone moieties in the dyads equipped with long linkages are able to bis-intercalate with the G4 structure whereas dyads that contain short linkages were unable to undergo such interaction. In addition, cationic dyads that contain long linkages are able to stabilize the quadruplex structure to a greater extent than dyads with shorter linkages.

1. Introduction

It has been well established that the single-stranded telomere segment at the 3′ ends of chromosomal DNA are able to form a variety of four-stranded structures known as G-quadruplexes (G4) *in vitro*, based on a G-tetrad structure of four Hoogsteen-paired, coplanar guanines (Fig. 1a). Such structures have been implicated in single-stranded telomeric DNA, which is a noncoding DNA found at the ends of linear eukaryotic chromosomes with a general sequence of tandemly repeated segments of between six to eight bases possessing guanine clusters. When the single-stranded 3′ end of a telomere folds into a G4 structure, it is no longer available to act as a primer for the enzyme telomerase [1]. Telomerase is deactivated in most somatic cells at birth, but in 85–90% of human tumors, it acts to extend telomere length, thus rescuing cells from crisis [2]. The potential application of G-quadruplexes to cancer treatment has been the driving force behind the investigation of ligands that stabilize G-quadruplexes and/or induce their formation [3–5]. Many small aromatic ligands, including porphyrins, quinacridones, anthraquinones, phenanthrolines, substituted triazines and acridines, have been shown to bind and stabilize the quadruplex structure of telomeric DNA. These ligands are capable of interactive stacking with the G-tetrads by a number of distinct mechanisms involving intercalation, end pasting or "sandwich"-type stacking, groove binding, or nonspecific external events involving charge neutralization [6–9].

To the best of our knowledge, despite various reports on the interaction of simple ligands with single binding sites of G4 structures, studies on the G4-interaction of complex dyads with multi-binding sites have not been reported. The present authors have previously reported the duplex-DNA binding modes of cationic porphyrin–anthraquinone (Por–Aq) dyads that comprised different lengths of flexible link; interestingly, the bridging linkage plays a key role in determining the DNA binding modes [10]. This paper investigates the binding modes of such cationic Por–Aq dyads using both absorption and fluorescence spectroscopy as well as surface-enhanced Raman spectroscopy (SERS) and induced circular dichroism (ICD); five alternative mechanisms are proposed to describe the nature of the binding of the dyads with the unique quadruplex structure.

* Corresponding author. MOE Laboratory of Bioinorganic and Synthetic Chemistry, School of Chemistry and Chemical Engineering, Sun Yat-Sen University, Xingangxi Road, Xin Gang Xi Lu, No. 135, Guangzhou, Guangzhou 510275, PR China. Fax: +86 20 84112245.
E-mail address: ceshjw@163.com (J.-W. Huang).

0143-7208/$ – see front matter © 2009 Elsevier Ltd. All rights reserved.
doi:10.1016/j.dyepig.2009.03.015

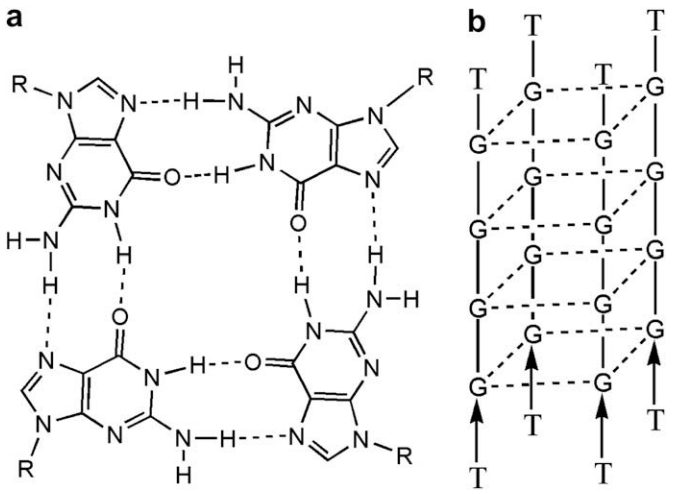

Fig. 1. Structure of a guanine quartet(a) and Schematic diagram of $(TG_4T)4$(b).

2. Experimental

2.1. Materials

The cationic Por–Aq dyads, **1**, **2**, **3** and **4** (see structures in Fig. 2) were synthesized and characterized in our laboratory [10]. Bromo acids with different lengths of carbon chain (such as 5-bromopentanoic or 8-bromooctanoic acid) were used to join Por and Aq moieties. Firstly, 1-amino-9, 10-anthraquione was linked to the bromo acid through an esterification; then a substitution reaction was carried out to join the 5-(4-hydroxyphenyl)-10, 15, 20-tris(4-N-pyridiniumyl)porphyrin and the carbon chain. At last the pyridinium groups on the porphyrin were methylated using methyl iodide. The purity of the final products was detected by NMR spectroscopy and elemental analysis (EA). These dyads were preserved in the dark under anhydrous conditions.

The DNA oligonucleotides TG_4T were purchased from the Shanghai Sangon Biological Engineering Technology & Services Co., Ltd. (China) in an HPLC-purified form. Single-strand extinction coefficients were calculated from mono- and dinucleotide data by a nearest-neighbor approximation method [11], using extinction coefficients at 260 nm of 57 800 M^{-1} cm^{-1}. The formation of intra- and inter-molecular G-quadruplexes was carried out as follows: the oligonucleotide sample TG_4T, dissolved in a KCl buffer solution (consisting of 10 mM Tris–HCl, 1 mM Na_2EDTA, and 100 mM KCl) was heated to 90 C for 5 min, gently cooled to room temperature, and then incubated at 4°C overnight. The formation of $(TG_4T)4$ was affirmed by the appearance of positive peak near 260 nm and shallow negative trough near 240 nm in CD spectra (Fig. S1 in supplementary materials), which is characteristic of parallel-stranded G-quadruplexes [12].

2.2. Methods

UV-Vis spectra were recorded on a Perkin-Elmer-Lambda-850 spectrophotometer. Emission spectra were recorded on a Perkin–Elmer Ls55 spectrofluorophotometer. SERS spectra were carried out on an inVia Laser Micro-Raman Spectrometer of Renishaw, with a power of 20 mW at the samples. CD spectra were recorded on a JASCO-J810 spectrometer.

2.2.1. SERS experiment

Ag colloids were prepared by reducing $AgNO_3$ with EDTA according to the reported method [13]. The Ag colloid/dyad (or Ag colloid/G4) SERS-active systems were prepared by mixing equal volume of the dyads (or G4) solution with the Ag colloid in Tris buffer to obtain the desired dyad or G4 concentrations. In the dyad/G4 complex experiments, the solution of G4 was mixed with the Por–Aq dyad solution at a G4/dyad ratio of 30:1, then an equal volume of the mixed solution was fully mixed with the Ag colloid, and the spectrum was immediately measured at room temperature. The final concentrations of dyads and G4 in all of the SERS-active systems were 5 and 150 μM, respectively.

2.2.2. Continuous variation analysis

A series of solution with varying mole fraction of Por–Aq dyad and $(TG_4T)4$ but the same sum concentration (30 μM) were used for this experiment, while the Por–Aq dyad solutions with corresponding concentrations were used as reference. Absorption difference spectra were collected from 350 to 500 nm with a 1 cm path-length quartz cell. For each spectrum collected, the Por–Aq dyad solution without an oligonucleotide was placed in the reference compartment and the corresponding Por–Aq dyad solution with an oligonucleotide was placed in the sample compartment. Cells were cleaned with concentrated HCl between measurements to remove all traces of Por–Aq dyad that easily deposits on the quartz cell. The difference in the maximum and minimum absorbance values was plotted versus the Por–Aq dyad mole fraction to generate a Job plot [14]. Linear regression analysis of the data was performed in the software of Origin 7.0.

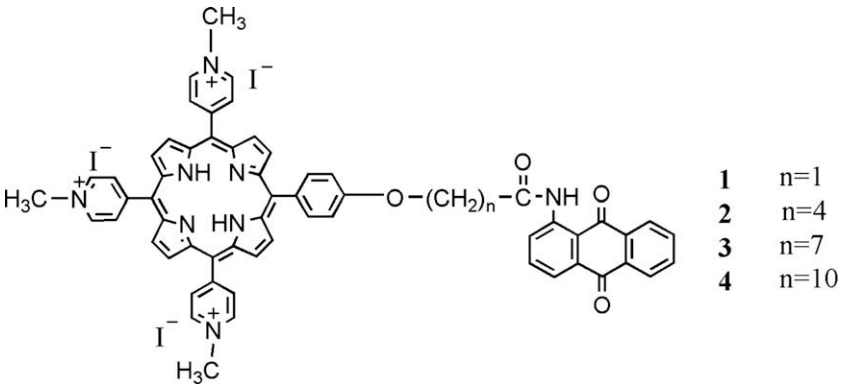

Fig. 2. Molecular structures of the cationic Por–Aq dyads.

3. Results and discussion

3.1. Absorption titrations

The association of the Por–Aq dyads with $(TG_4T)4$ was examined by absorption titration in the UV–Vis range. Fig. 3 exemplifies the absorption spectral changes of **2** upon $(TG_4T)4$ addition and those of **1**, **3** and **4** are available in the supplementary materials as Fig. S2. Table 1 summarizes the detailed titration data of all these Por–Aq dyads at both Por and Aq's absorption bands.

In the case of duplex DNA as a host, porphyrin intercalation is characterized experimentally by a large bathochromic shift ($\Delta\lambda \geq 10$ nm) and substantial hypochromicity ($H \geq 35\%$) of the Soret band. On the other hand, the external binding mode of porphyrins is characterized by a small bathochromic shift ($\Delta\lambda \leq 8$ nm) and hypochromicity ($H \leq 10\%$) [8,10,15,16]. In Table 1, for **3** and **4**, the observed $\Delta\lambda$ (11–12 nm) and H (46.2–48.6%) values at the porphyrin's Soret bands suggest that the porphyrin planes in these two dyads may intercalate into G4 structures. In fact, previous results have indicated that the red shifts (≥10 nm) and hypochromicities (≥35%) given for intercalative binding modes were determined for long segments of duplex DNA, where end stacking is not significant [15]. This is a great difference between duplexes and quadruplexes in studying small molecule binding modes [14,16,17]. Thus, the results of the absorbance titration indicate the intense interaction between the dyads and G4, whereas a conclusion as to the specific binding mode of these Por–Aq dyads cannot be made from this method alone.

It is interesting to find that the $\Delta\lambda$ and H values at both Por and Aq's absorption bands for dyads with long linkages were larger than those for **2** with shorter bridging links of four flexible methylenes, while those for **1** with only one methylene are the smallest. This phenomenon is similar to the absorption changes of these dyads with the titration of duplex DNA [10]. We believe that the different absorption change in the case of duplex DNA were mainly attributed to the different DNA binding modes of these dyads, in which a larger change corresponding to a better binding mode [10]. Thus, it is supposed that these Por–Aq dyads bind with $(TG_4T)4$ in different modes, and the dyads with longer linkages may employ more beneficial binding modes than those with shorter bridging links.

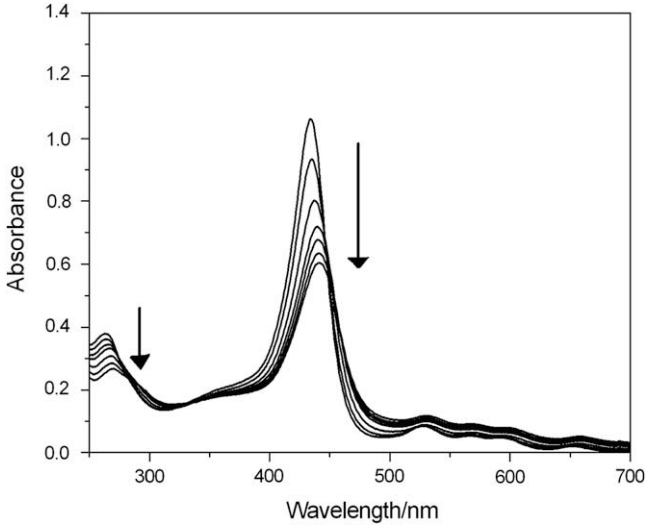

Fig. 3. Absorption spectrum of the **2** in KCl buffer at 25 °C in the presence of increasing amounts of $(TG_4T)4$. [Por] = 10 μM. Additions range from 0 to 20 μM. Arrows indicate the change in absorbance upon increasing the DNA concentration.

3.2. Fluorescence studies

Fluorescence titration experiments of the Por–Aq dyads in the presence of G4 were performed. Fluorescence emission spectral changes of these dyads with increasing $(TG_4T)4$ were shown in Fig. 4. From Fig. 4, it can be seen that the fluorescence intensities of all these Por–Aq dyads at the porphyrin characteristic emission band (*ca.* 665 nm) are remarkably enhanced with the increase of $(TG_4T)4$. Meanwhile, for **2**, **3** and **4**, the fluorescence intensities at *ca.* 370 nm ascribed to the Aq moieties of the dyads, are also clearly observed to increase with addition of G4 DNA. Since the hydrophobic environment provided by G4 structures can protect small molecules from quenching by water molecules, the emission increase is widely admitted as an indication of the interaction between small molecules and G4 structures [18,19]. Thus, the significant increases in both Por's and Aq's emission ranges suggest that both Por and Aq planes in **2**, **3** and **4** probably bind with $(TG_4T)4$ in an intercalative binding mode. However, in the case of **1**, no clear fluorescence increase is observed in the Aq emission range, suggesting that G4 binding affinity of the Aq moiety in **1** may be not so large and a non-intercalative binding mode is probably employed.

3.3. SERS investigation

SERS is a powerful tool for the study of the interactions of drugs, especially fluorescence molecules, with biomacromolecules at very low concentrations. The silver colloids can be adapted for the application in the study of biological objects, because they do not modify to a great extent the structures of biological molecules adsorbed on their surface [20]. To further clarify the binding modes of these Por–Aq dyads to G4 DNA, SERS spectra were measured.

The SERS spectra of $(TG_4T)4$ and the dyads in the absence and presence of G4 DNA are shown in Fig. 5. The bands centered at 411–1141 cm^{-1} are attributed to the Por ring and those centered at 1442, 2946 cm^{-1} can be ascribed to the carbon links in the molecule [10]. It is found that no substantial SERS signal is given by $(TG_4T)4$, since the Ag colloids have negative charges on their surface, which repels the adsorption of negatively-charged DNA molecules [21].

Curves a–d in Fig. 5 show the SERS spectra of the dyads in the absence of $(TG_4T)4$, which are very similar to each other. This similarity in the SERS spectra results from the quite similar molecular structure of these dyads. Curves a'–d' in Fig. 5 show the SERS spectra of complexes of Por–Aq dyads at 5 μM with $(TG_4T)4$ at 150 μM. SERS spectra of these dyads in the presence of $(TG_4T)4$ are also quite similar to each other but very different from those in the absence of G4 DNA. Most bands of the hybrid/G4 complexes disappear, indicating that the interactions of Por–Aq dyads with $(TG_4T)4$ can largely reduce the amount of dyads adsorbed on Ag colloids [22]. Especially, the disappearance of the band at 330 cm^{-1}, which is mainly assigned to the bending

Table 1
Physical data of Por–Aq dyads binding with $(TG_4T)4$.

Dyads	UV–Vis		Spectra		ICD	Spectra	ΔT_m
	Por		Aq		Por (mdeg)		
	Δλ(nm)	H%	Δλ(nm)	H%	+	–	°C
1	2	30.1	1	20.1	1.6	1.8	3.0
2	8	43.1	7	29.5	3.1		6.4
3	12	48.6	9	33.1		2.6	12.8
4	11	46.2	10	35.88		3.0	11.2

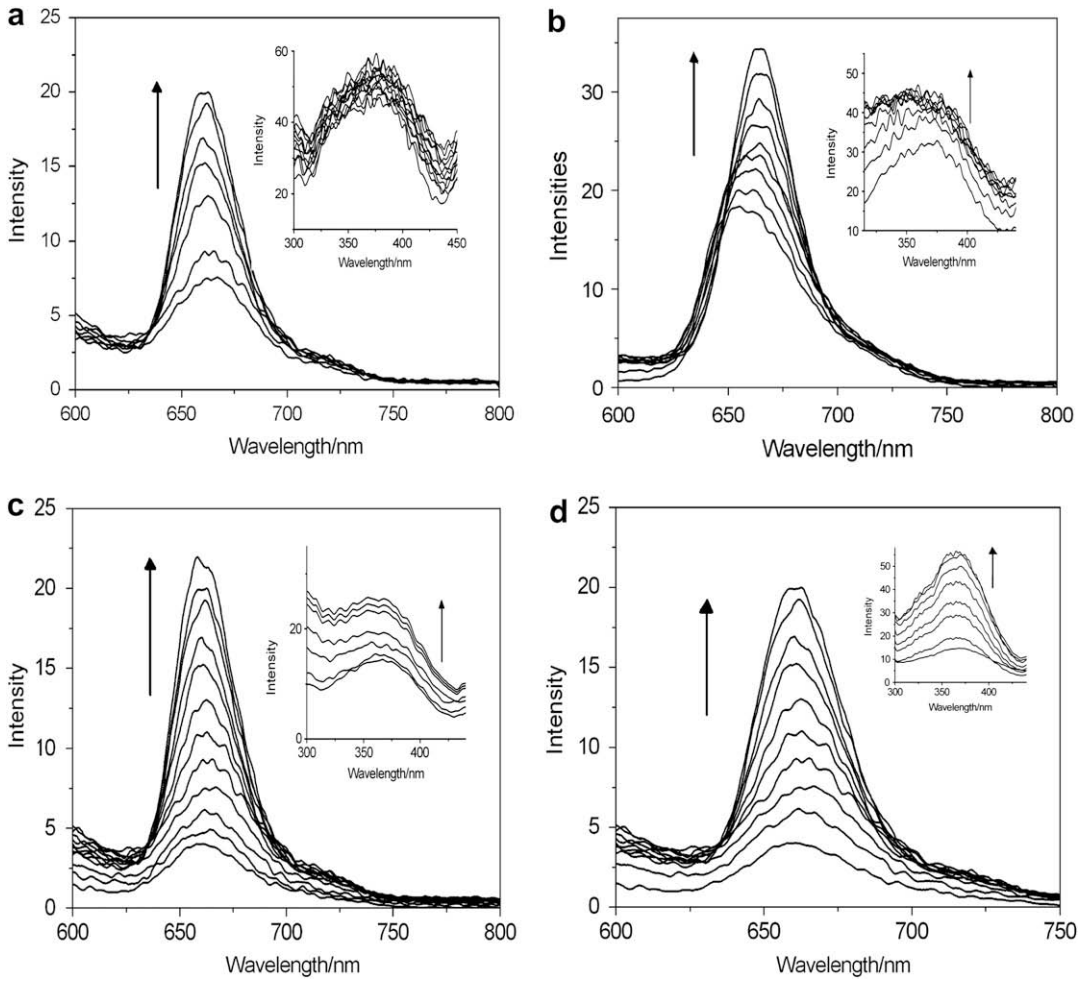

Fig. 4. Emission spectra for Por moieties of **1** (a), **2** (b), **3** (c) and **4** (d) in KCl buffer at 25 °C in the absence and presence of $(TG_4T)4$ DNA. [Por] = 10 μM. Additions range from 0 to 20 μM. Arrows show the intensity change upon increasing G4 concentrations. (Inset: the emission for Aq moieties of dyads, respectively).

vibration of Por and is the marker band of the free-base Por in the SERS-active system [21–23], indicates the loss of free-base Por molecules surrounding Ag colloids after the interaction between Por–Aq dyads and $(TG_4T)4$. The disappearance of bands centered at 411, 814, 965, 1001, 1098, 1141 cm^{-1} which are attributed to the Por ring, also proves that the Por moieties of the dyads are protected by $(TG_4T)4$ structures from adsorbing on Ag particles. The band at 1554 cm^{-1} which is the characteristic band of anthracene dyads vanishes [24], indicating that the Aq moieties of the dyads are embedded in G4 DNA molecules. However, the remaining of bands centered at 1442, 2946 cm^{-1}, which can be ascribed to the carbon links in the molecule [24], suggests that the flexible carbon links may be still exposed in the solvent when the two planar moieties are well protected by the G4 structure. In summary, all of these changes in the SERS intensities are ascribed to the intense interactions between the Por–Aq dyads and $(TG_4T)4$.

Moreover, the chosen protocol for the SERS sample preparation allows the G4-hybrid adduct to be formed before its addition to the colloid solution (see Experimental). Consequently, the spectral changes confirm that the Por–Aq hybrid efficiently binds to G4 DNA even in Ag sols. In this medium, the preference of cationic hybrid for polyanionic G4-DNA prevails over negatively-charged Ag nanoparticles [25,26]. This also reveals the tight binding affinities between the cationic dyads and G4 DNA.

3.4. ICD spectra

It has been reported that the ICD spectra in the Soret region of porphyrins are well-defined indicators for the binding modes toward duplex DNA. A positive ICD peak is due to groove binding and a negative ICD peak is due to intercalative binding, whereas a bisignate ICD peak is ascribed to the external self-stacking binding mode of porphyrins to DNA [15,27–29]. This criterion is also applicable in the interaction of porphyrins with G4 structures [17,30].

Fig. 6 illustrates the ICD spectra and Table 1 lists the physical data for porphyrin dyads in the presence of $(TG_4T)4$. None of these dyads as well as $(TG_4T)4$ by themselves displays any CD spectra signal in the visible region, but ICD spectra are observed in the Soret band of these porphyrin dyads upon DNA titration. The ellipticities observed for **3** and **4** in the presence of G4 DNA are predominantly negative in character and centered in the wavelength ranging from 400 to 500 nm. Since the negative ICD signal is diagnostic of intercalative binding, this result confirms that the Por moieties of **3** and **4** intercalate into the $(TG_4T)4$ structure under the experimental conditions. However, the substantial bisignate ICD signal for **1** and positive ICD band for **2** provide evidence that the Por moieties of these two dyads bind to $(TG_4T)4$ in external self-stacking and groove binding modes, respectively. The distinct ICD signals of these dyads are in good agreement with the foregoing experimental results.

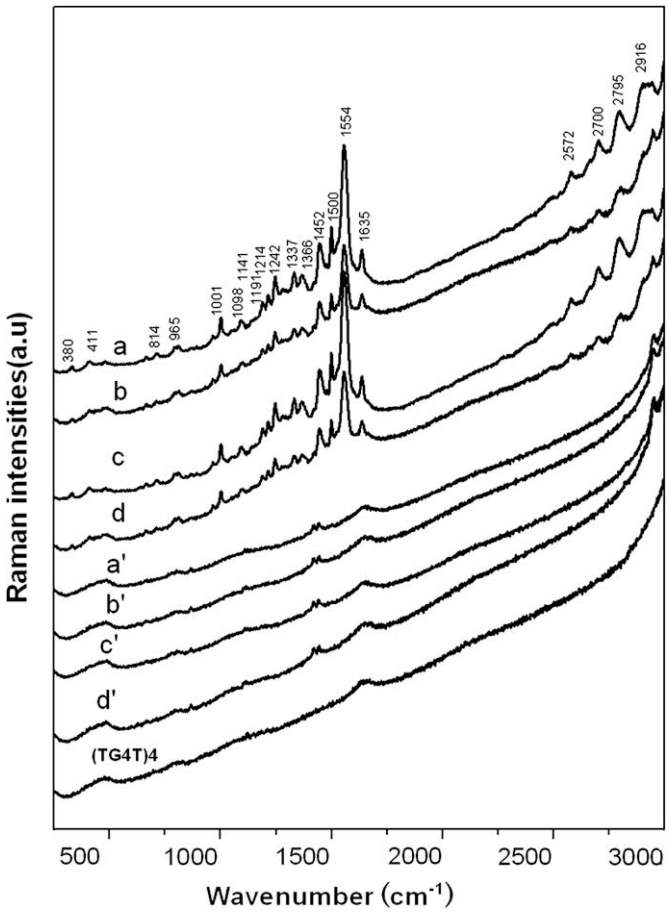

Fig. 5. SERS spectra (300–3000 cm^{-1}) Por–Aq dyads in the absence (a–d) and presence (a'–d') of (TG_4T)4. (a)–(d) for free **1**, **2**, **3** and **4**, respectively; (a')–(d') for G4 complexes with **1**, **2**, **3** and **4**, respectively. [G4]/[Por] = 30:1.

3.5. Job plots

To further identify and obtain exact numbers of ligand-binding sites, the method of continuous variation analysis (Job plot) was used. The points of the intersection of two best fit lines in the Job plots (Fig. 7) for the complexes of Por–Aq with (TG_4T)4, are 0.65, 0.67, 0.70 and 0.63, corresponding to Por–Aq/G4 stoichiometric ratios of 1.8:1, 2.0:1, 2.3:1 and 1.7:1 for **1**, **2**, **3** and **4**, respectively. Thus, the number of molecules binding per quadruplex of all the Por–Aq dyads is determined to be 2. The different spectra used to generate the Job plots, are available in the Supporting Information as Fig. S3.

Based on the results of spectral experiments above and the job plots, the G4 DNA binding modes of these Por–Aq dyads were proposed, as shown in Fig. 8. In investigating the binding modes of these Por–Aq dyads with duplex DNA, it has been experimentally and theoretically proved that the Por–Aq dyads with longer flexible bridging links, **2**, **3** and **4**, could interact with duplex DNA in a bis-intercalative mode while **1** with short linkage suffers severe steric hindrance in DNA binding [10]. From the above results of G4 interacting, it is likely that, similar to the binding with duplex DNA, the Por and Aq moieties in **1** and **2** suffer steric hindrance from each other, while those in **3** and **4** could independently interact with DNA and both are sterically appropriate to bind with (TG_4T)4 in intercalative mode.

3.6. Thermal denaturation studies

The melting curves of (TG_4T)4 in the absence and presence of dyads are presented in Fig. 9. Under the present experimental conditions, the melting curve has a transition, and the T_m value of free (TG_4T)4 is (56.2 ± 0.2)°C; when mixed with the dyads, the observed melting temperatures of G4 DNA increase to different extents and the increases of T_m (ΔT_m) are summarized in Table 1.

It has been reported that the telomerase inhibition of drugs was strongly related to the stabilization of the quadruplex structure [30,31]. From Table 1, it can be found that the values of ΔT_m in the presence of these Por–Aq dyads are relatively large, (3.0–12.8 °C), indicating that the dyads contribute to the stabilization of the quadruplex structure. Noteworthy is the fact that the

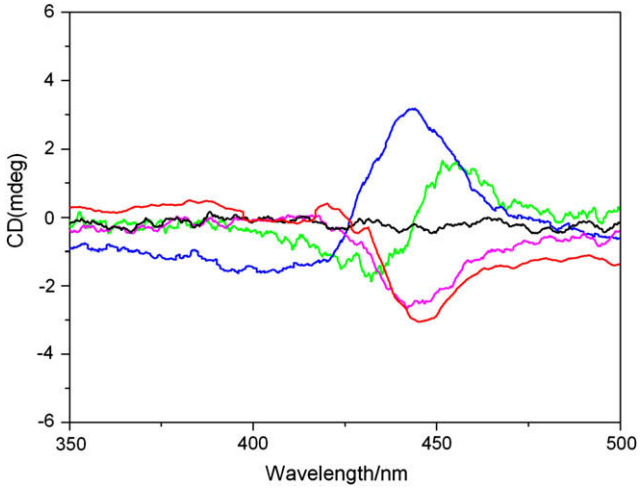

Fig. 6. Induced CD spectra of porphyrins in the absence (—) and presence of (TG_4T)4 in KCl buffer. **1**(—), **2** (—), **3**(—) and **4**(—), [Por] = 10 μM, [G4] = 25 μM.

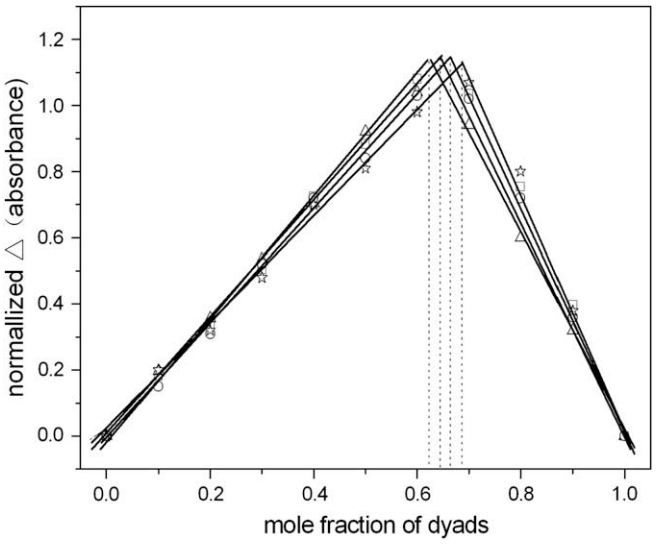

Fig. 7. Job plots for the binding of **1** (□), **2** (○), **3** (☆) and **4** (△) to (TG_4T)4 in KCl buffer 1.

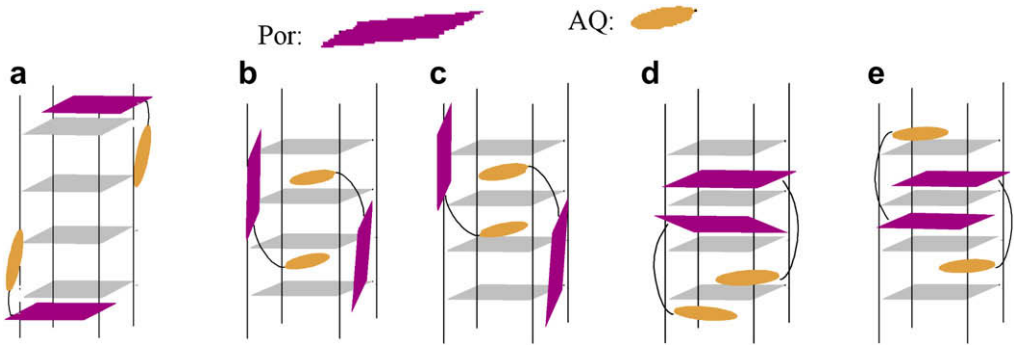

Fig. 8. Supposed binding modes of cationic Por-Aq dyads to $(TG_4T)4$: (a) for **1**; (b) and (c) for **2**; (d) and (e) for **3** and **4**.

Por–Aq dyads with longer links were much more effective in the stabilization of the quadruplex structure than those with shorter bridging links. Since the proposed binding modes in Fig. 7 suggests that only the porphyrin rings in the long bridging dyads intercalate into the G-quadruplex structures, it is suggested that the cationic porphyrin ring may contribute more than the Aq ring in stabilizing the G4 structures. This may result from two reasons: (1) the dimensions of this cationic porphyrin ring are roughly similar to those of a G-tetrad; (2) the porphyrin ring has constituents that can hydrophobically and electrostatically interact with a G-tetrad [17].

4. Conclusion

In this report, we have proposed the G-quadruplex binding modes of Por–Aq dyads with multi-binding sites through spectroscopic methods and Job plot research. As revealed by the increase of melting temperature of G4, the dyads with long linkages, whose porphyrin rings intercalate into G4 structures, could stabilize the parallel quadruplex DNA $(TG_4T)4$ better than those with shorter linkages, whose porphyrin rings bind with G4 structures in non-intercalative modes. It seems that the intercalation of the cationic porphyrin rings in the Por–Aq dyads is very significant in the efficient stabilization of quadruplex DNA structure. This study takes the lead in researching the binding and stabilization to G-quadruplex of complex dyads with multi-binding sites, and may provide insight into the structural change of G-quadruplex upon binding of ligands.

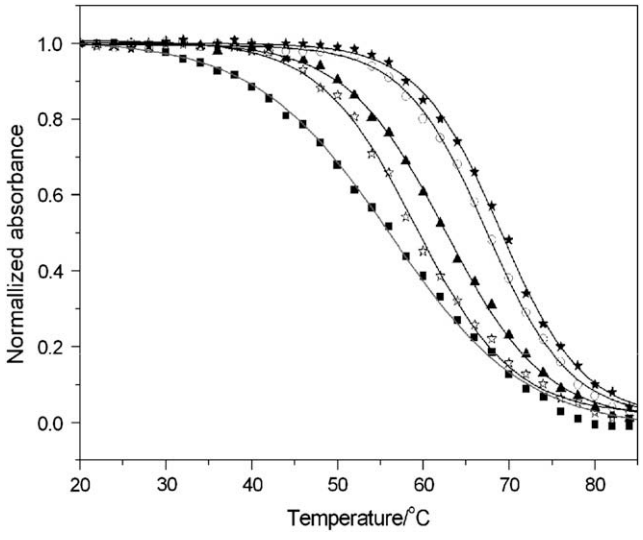

Fig. 9. Melting curves of $(TG_4T)4$ in KCl buffer 2 at 295 nm in the absence (■) and the presence of **1** (□), **2** (▲), **3** (□) and **4** (○) in KCl buffer 2. [Por] = 20 μM, [G4] = 40 μM.

Acknowledgements

This work was financially supported by the three following units of the People's Republic of China: the National Natural Science Foundation (29971034, 20071034, 20231010), the N.S.F. of Guangdong Province and Guangzhou Municipality Science & Technology Bureau.

Appendix. Supplementary material

Supplementary material associated with this article can be found, in the online version, at doi:10.1016/j.dyepig.2009.03.015.

References

[1] Read MA, Neidle S. Structural characterization of a guanine–quadruplex ligand complex. Biochemistry 2000;39:13422–32.
[2] Cech T. Life at the end of the chromosome: telomeres and telomerase. Angewandte Chemie International Edition 2000;39:34–43.
[3] Parkinson GN, Lee MPH, Neidle S. Crystal structure of parallel quadruplexes from human telomeric DNA. Nature 2002;417:876–80.
[4] Han H, Langley DR, Rangan A, Hurley LH. Selective interactions of cationic porphyrins with G-quadruplex structures. Journal of the American Chemical Society 2001;123:8902–13.
[5] Vialas C, Pratviel G, Meunier B. Oxidative damage generated by an oxo-metalloporphyrin onto the human telomeric sequence. Biochemistry 2000;39:9514–22.
[6] Heald RA, Modi C, Cookson JC, Hutchinson I, Laughton CA, Gowan SM, et al. Antitumor polycyclic acridines. 8. Synthesis and telomerase-inhibitory activity of methylated pentacyclic acridinium salts. Journal of Medicinal Chemistry 2002;45:590–7.
[7] Sun D, Thompson B, Cathers BE, Salazar M, Kerwin SM, Trent JO, et al. Inhibition of human telomerase by a G-quadruplex-interactive compound. Journal of Medicinal Chemistry 1997;40:2113–6.
[8] Wheelhouse RT, Sun D, Han H, Han FX, Hurley LH. Cationic porphyrins as telomerase inhibitors: the interaction of tetra-(N-methyl-4-pyridyl)porphine with quadruplex DNA. Journal of the American Chemical Society 1998;120:3261–2.
[9] Gavathiotis E, Heald RA, Stevens FG, Searle MS. Recognition and stabilization of quadruplex DNA by a potent new telomerase inhibitor: NMR studies of the 2:1 complex of a pentacyclic methylacridinium cation with d(TTAGGGT)4. Angewandte Chemie International Edition 2001;40(2):4749–51.
[10] Zhao P, Xu LC, Huang JW, Fu B, Yu HC, Zhang WH, et al. DNA-binding and photocleavage properties of cationic porphyrin–anthraquinone dyads with different lengths of links. Bioorganic Chemistry 2008;36:278–87.
[11] Cantor CR, Warshaw MW, Shapiro H. Oligonucleotide interactions. III. Circular dichroism studies of the conformation of deoxyoligonucleotides. Biopolymers 1970;9:1059–77.
[12] Keniry MA. Quadruplex structures in nucleic acids. Biopolymers 2001;56:123–46.
[13] Sergei NT, Victor AG, Vladimir SC, Pierre-Yves T. Resonance Raman and absorption characterization of cationic Co(II)–porphyrin in its complexes with nucleic acids: binding modes, nucleic base specificity and role of water in Co(II) oxidation processes. Journal of Raman Spectroscopy 2005;36:962–73.

[14] Keating LR, Szalai VA. Parallel-stranded guanine quadruplex interactions with a copper cationic porphyrin. Biochemistry 2004;43:15891–900.
[15] Pasternack RF, Gibbs EJ, Villaffranca JJ. Interactions of porphyrins with nucleic acids. Biochemistry 1983;22:2406–14.
[16] Haq I, Trent JO, Chowdhry BZ, Jenkins TC. Intercalative G-tetraplex stabilization of telomeric DNA by a cationic porphyrin. Journal of the American Chemical Society 1999;121:1768–79.
[17] Anantha NV, Azam M, Sheardy RD. Porphyrin binding to quadruplexes T4G4. Biochemistry 1998;37:2709–14.
[18] Trommel S, Marzilli LG. Synthesis and DNA binding of novel water-soluble cationic methylcobalt porphyrins. Inorganic Chemistry 2001;40:4374–83.
[19] Ji LN, Zou XH, Liu JG. Shape and enantioselective interaction of Ru(II)/Co(III) polypyridyl complexes with DNA. Coordination Chemistry Reviews 2001;216-217:513–36.
[20] Groot JD, Hester RE. Surface-enhanced resonance Raman spectroscopy of oxyhemoglobin adsorbed onto colloidal silver. Journal of Physical Chemistry 1987;91:1693–6.
[21] Wei CY, Jia GQ, Yuan JL, Feng ZC, Li C. A spectroscopic study on the interactions of porphyrin with G-quadruplex DNAs. Biochemistry 2006;45:6681–91.
[22] Procházka M, Turpin PY, Sÿtěpánek J, Bok J. SERRS spectra of azo dyes from deposited Ag colloid-azo dye films: investigating the mechanism of film formation. Journal of Molecular Structure 1999;482-483:221–4.
[23] Terekhov SN, Kruglik SG, Malinovskii VL, Galievsky VA, Chirvony VS, Turpin PY. Resonance Raman characterization of cationic Co(II) and Co(III) tetrakis(N-methyl-4-pyridinyl)porphyrins in aqueous and non-aqueous media. Journal of Raman Spectroscopy 2003;34:868–81.
[24] Ning YC. In: Hu RG, editor. Structure identification of organic compounds and organic spectroscopy. Science Press: Inc.; 1991. p. 485–98.
[25] Gaudry E, Aubard J, Amouri H, Le′ vi1 G, Cordier C. SERRS study of the DNA binding by Ru(II) tris-(bipyridyl) complexes bearing one carboxylic group. Biopolymers 2006;82:399–404.
[26] Hanzlıková J, Procházka M, Sÿtěpánek J, Bok J, Baumruk V, Anzenbacher PJ. Metalation of 5,10,15,20-tetrakis(1-methyl-4-pyridyl)porphyrin in silver colloids studied via time dependence of surface-enhanced resonance Raman spectra. Journal of Raman Spectroscopy 1998;29:575–84.
[27] Zhao P, Xu LC, Huang JW, Fu B, Yu HC, Ji LN. Tricationic pyridium porphyrins appending different peripheral substituents: experimental and DFT studies on their interactions with DNA. Biophysical Chemistry 2008;135:102–9.
[28] Zhao P, Xu LC, Huang JW, Fu B, Yu HC, Ji LN. DNA binding and photocleavage properties of a novel cationic porphyrin–anthraquinone hybrid. Biophysical Chemistry 2008;134:72–83.
[29] Zhao P, Xu LC, Huang JW, Fu B, Yu HC, Ji LN. Experimental and DFT studies on DNA binding and photocleavage of two cationic porphyrins: effects of the introduction of a carboxyphenyl into pyridinium porphyrin. Spectrochimica Acta Part A: Molecular and Biomolecular Spectroscopy 2008;71:1216–23.
[30] Takeshi Y, Tadayuki U, Yoshinobu I. Stabilization of guanine quadruplex DNA by the binding of porphyrins with cationic side arms. Bioorganic & Medicinal Chemistry 2005;13:2423–30.
[31] Shi S, Liu J, Yao TM, Geng XT, Jiang LF, Yang QY, et al. Promoting the formation and stabilization of G-quadruplex by dinuclear RuII complex $Ru_2(obip)L_4$. Inorganic Chemistry 2008;47(8):2910–2.